Chapter 7

Colloidal Interactions in Ionic Liquids—The Electrical Double Layer Inferred from Ion Layering and Aggregation

Rosa M. Espinosa-Marzal,[*,1,2] Zachary A. H. Goodwin,[*,3,4] Xuhui Zhang,[1] and Qianlu Zheng[1]

[1]Civil & Environmental Engineering, University of Illinois at Urbana-Champaign, Illinois 61801, United States

[2]Materials Science & Engineering, University of Illinois at Urbana-Champaign, Illinois 61801, United States

[3]John A. Paulson School of Engineering and Applied Science, Harvard University, Cambridge, Massachusetts 02138, United States

[4]Department of Materials, Imperial College London, London SW7 2AZ, UK

[*]Email: rosae@illinois.edu

[*]Email: zachary.goodwin13@imperial.ac.uk

Ionic liquids (ILs) are organic salts that remain liquid in absence of a solvent over a wide range of temperatures, often at room temperature. This chapter summarizes the progress in understanding colloidal interactions mediated by ILs and their electrical double layer (EDL) based on experimental observations and theory. It is well known that short-range oscillatory forces in ILs originate from the overscreening provided by ion layers that accumulate close to the charged surface. In contrast, the origin of the more surprising long-range decaying force is not well understood yet. There is experimental and theoretical evidence opposing the originally proposed dilute behavior of ILs, arising from either ion pair formation or solvent/voids/alkyl tails being the effective charge carrier. Here, we overview experiments and theory that supports an alternative explanation of this long-range force based on ion aggregation.

Introduction

Ionic liquids (ILs) are organic salts with low melting points (*1*–*3*). That is, they are composed solely of anions and cations –making them highly concentrated electrolytes– with at least one of the ions being large, polyatomic, and non-uniformly charged (*1*). The large size of the ions, often with flexible and/or asymmetric molecular structures, introduces large conformational and configurational entropy, and weakens the electrostatic correlations between ions. These characteristics hinder the formation of crystal lattices, which results in a low liquidus temperature,

Nagarajan; One Hundred Years of Colloid Symposia: Looking Back and Looking Forward
ACS Symposium Series; American Chemical Society: Washington, DC, 2023.

often below room temperature (*1*). ILs have generated great excitement in energy storage research, in large part thanks to their wide electrochemical stability window and chemical tunability (*1*, *4*–*7*). In the last decade, research on the interfacial behavior of ILs has become one of the fastest-moving fronts in interfacial science (*6*, *7*). Moreover, the design versatility and tunable properties enable their application in a variety of other areas, including lubrication (*8*), and catalysis (*9*).

Colloidal interactions mediated by electrolytes not only play a central role in many fields of application such us nanoceramics fabrication, water treatment, food industry, as well as in biological research (*10*), but also provide fundamental insight into the properties of the electrolyte. Horn's pioneering force measurements using a surface forces apparatus in a protic IL, ethyl ammonium nitrate (EAN), demonstrated the arrangement of ethyl ammonium and nitrate ions in molecular layers in close proximity to the atomically smooth and negatively charged surface (mica) (*11*). About twenty years later, Atkin and Warr revealed molecular layers at the interface between protic and aprotic ILs, and mica, silica and graphite (*12*). Shortly later, Metzger *et al.*'s synchrotron X-ray reflectivity measurements probed the oscillatory electron density profile of two aprotic ILs on a sapphire surface with Å resolution (*13*). Since then, many more studies have proved that ions arrange in layers at smooth IL-solid interfaces (see review in ref. (*8*)).

In 2013 (*14*), the measurement of colloidal forces in ILs, which decay exponentially from a charged surface with a length scale (~10 nm) that is orders of magnitude larger than the expected Debye length for a highly concentrated electrolyte (~0.1 nm), surprised the interfacial science community and challenged the broadly accepted paradigm of electrical double layers in superconcentrated electrolytes (*15*–*17*). These forces have been assumed to be of electrostatic origin and their large decay length has been postulated to originate from a renormalization of the charge carrier concentration and to obey a scaling law with the permittivity of the liquid and temperature (*18*). However, the origins of this renormalization are not well-understood, and in fact, directly contradicts many other experimental measurements (*15*). An emerging consensus is that non-electrostatic intermolecular forces also play a crucial role, and that their interplay with the electrostatic forces leads to the formation of rich mesoscale structures that determine the surface mediated interactions. This chapter describes this emerging consensus.

Experimental Observations

This section is organized as follows. We first describe the short-range structural (solvation) force mediated by ILs, and how the solvation layers inferred from them respond to an applied potential. Next, we summarize the main findings with regard to the long-range surface forces, initially thought to be the electrostatic double layer force of a dilute electrolyte. We conclude this section with additional experimental observations that provide evidence for an alternative origin of this long-range force.

Short-Range Structural (Solvation) Forces Mediated by ILs

Using a Surface Forces Apparatus (SFA), Horn *et al.* studied the surface forces mediated by ethylammonium nitrate (EAN) and its mixtures with water, between two mica sheets (*11*). As expected, the surface forces for dilute solutions of EAN in water are well described by the DLVO theory (*19*) (Figure 1a). That is, the decay length of the electrical double layer force agrees well with the Debye length determined by the Debye-Hückel theory for a dilute electrolyte. As the concentration is increased, the change in the force curves was described in the context of counterion

adsorption (cation binding to a negatively charged surface) according to the ion-exchange model proposed by Pashley (*20*), and revised by Miklavic and Ninham (*21*). That is, cation adsorption in the Stern layer reduces the effective surface charge, and thereby, the length scale of the interactions. Based on this model, at concentrations of ~ 1 M, the effective surface charge becomes negligible, and the electrical double-layer repulsion becomes so short-ranged that the overall surface force is dominated by the van der Waals attraction (Figure 1b).

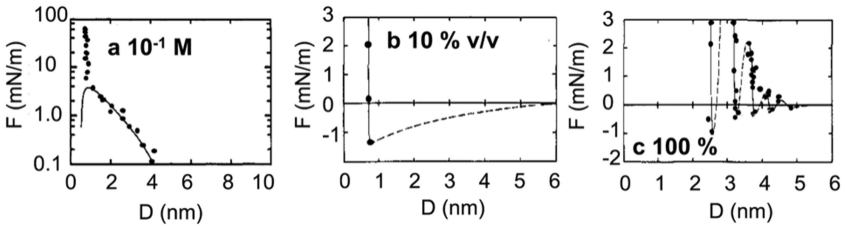

Figure 1. Surface forces between mica surfaces in EAN at various concentrations in water: (a) 0.1 M, (b) 10% w/v (1 M) EAN in water, (c) pure EAN (11.2 M). Adapted with permission from reference (*11*). *Copyright 1988 American Chemical Society.*

These pioneering force measurements also showed that, at volume fractions of EAN larger than 50% (5.7 M), the force profile becomes oscillatory. The spacing of the oscillations was determined to be ~ 0.5-0.6 nm, independently on the concentration. More oscillations were measured as the volume fraction of EAN increased. For pure EAN (100%, 11.2 M), the force profile showed 8-9 oscillations upon approach of the surfaces from a distance of ~ 5 nm (Figure 1c). This short-range structural force is similar to the solvation force found in nonpolar solvents that organize in molecular layers at the solid-liquid interface. The size of the oscillations is also close to the size of an ion pair, and hence, they point at the formation of molecular/ion layers –often referred as solvation layers– in the proximity of the mica surfaces, which are squeezed out as the surfaces approach each other.

Atomic Force Microscopy (AFM) was used several years later by Atkin *et al.* to measure the force between Si_3N_4 tips and various surfaces (mica, silica, and graphite) in three room-temperature ILs (*12*); see example in Figure 2a. The force revealed an oscillatory component, with the size of the oscillations corresponding to the dimension of the ion pair, in qualitative agreement with Horn's measurements. The comparison of force-distance curves revealed that surface charge, roughness and molecular structure of the IL influences the formation and characteristics of the ion layers, *i.e.*, surface charge promotes layering, while roughness disturbs it. Thus, the greatest number of interfacial (solvation) layers with EAN was observed on highly charged, atomically smooth mica. An increase in IL flexibility via longer alkyl chains (*e.g.*, propyl ammonium instead of ethyl ammonium) led to fewer and more compressible layers. Stronger layers were found to form on graphite with IL ions that had longer alkyl groups, since they enhance the attractive interactions with the surface. The orientation of the ions also affected interfacial layering, *e.g.*, imidazolium cations adopt a flat orientation on graphite to maximize the interaction between the surface and the alkyl group which significantly promotes the formation of ion layers. Fewer layers were detected on mica and silica because imidazolium cations are orientated with the ethyl group facing the bulk due to electrostatic interactions with these charged surfaces.

IL-mediated surface forces were also investigated by Perkin *et al*. using a surface force balance (SFB (*24*), similar to SFA (*25*)) and 1-ethyl-3-methyl imidazolium ethylsulphate (abbreviated as

$[C_2C_1Im][EtSO_4]$) (*22*). These measurements were in agreement with Horn's earlier measurements and confirmed the oscillatory nature of the short-range interaction – also called oscillatory structural force or simple structural force– between mica surfaces (Figure 2b). These studies also demonstrated that, in the regime of low pressures (<1 MPa), the coefficient of friction –i.e. the ratio between friction force and normal load– is 1–2 orders of magnitude smaller than for analogous thin films of non-polar molecular liquids, including standard hydrocarbon lubricants. It thus appears that the confined films of ILs are sufficiently robust under shear due to the strong coulombic interactions between ions and the surface, and they remain confined between the surfaces at high applied pressures. For more information about the behavior of ILs under shear and their tribological properties, we refer the readers to a review by Espinosa-Marzal *et al*. (*8*).

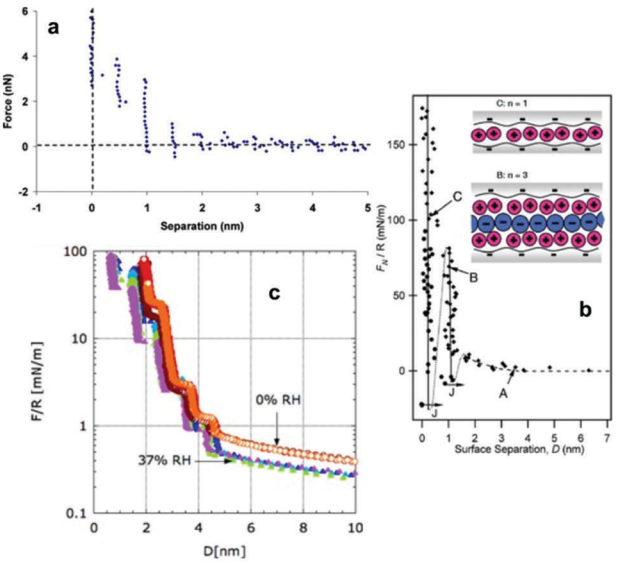

Figure 2. (a) Surfaces forces measured with an AFM tip approaching a mica surface in EAN. Adapted with permission from reference (*12*)*. Copyright 2007 American Chemical Society. (b) Surface forces between mica surfaces in $[C_2C_1Im][EtSO_4]$ measured by SFB. Reproduced with permission from reference* (*22*)*. Copyright 2010 Royal Society of Chemistry. (c) Surface forces between mica surfaces in $[C_2C_1Im][FAP]$ at 0 and 37% RH. Abbreviations: FAP = tris(pentafluoroethyl)trifluorophosphate. Adapted with permission from reference* (*23*)*. Copyright 2014 American Chemical Society.*

When ILs are exposed to humid air, they absorb water. The first studies of the influence of water uptake on the colloidal forces mediated by ILs were carried out in 2014 by Espinosa-Marzal *et al*. using an extended SFA (*23*, *26*). The extended SFA (abbreviated eSFA) is a fully automatized instrument with higher thermal and mechanical stability than conventional SFAs (*27*). The eSFA also has a greater precision in distance measurement (~25 pm) than conventional SFAs due to the use of a numerical method –fast spectral correlation– to evaluate the transmitted interference signal. In an eSFA, the mica surfaces approach at constant velocity very slowly (~1-3 Å/s) and the oscillatory component of the force appears as a step in the force profile, like in AFM measurements. These measurements showed, for various hydrophilic and hydrophobic ILs, that the enrichment of water molecules at the IL/mica interface influences both the layered structure of the nanoconfined IL, the

force (Figure 2c), and the dynamics of the squeeze-out of the layers. Interfacial water appears to change both the ion-pair orientation and the slip condition for the squeeze out of layers (so-called film-thickness transitions), that is, the resistance of the IL layers against being squeezed out.

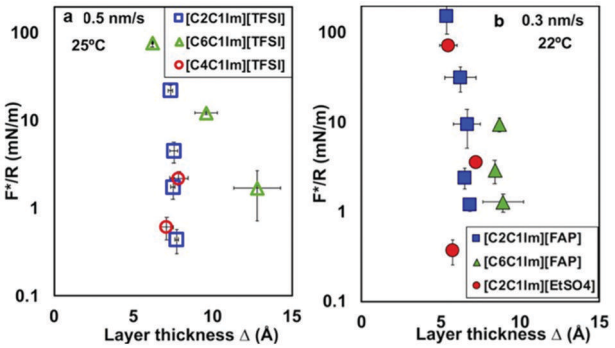

Figure 3. Layer sizes and force applied to squeeze out IL layers in (a) $[C_2C_1Im][TFSI]$, $[C_4C_1Im][TFSI]$ and $[C_6C_1Im][TFSI]$ and (b) $[C_2C_1Im][FAP]$, $[C_6C_1Im][FAP]$ and $[C_2C_1Im][EtSO_4]$. Abbreviation: 1-n-alkyl 3-methylimidazolium $[C_nC_1Im]^+$, with n = 2, 4 and 6 for ethyl, butyl and hexyl, respectively; [TFSI] = bis(trifluoromethanesulfonyl)imide. Adapted with permission from reference (28). Copyright 2018 American Chemical Society.

The thickness of the interfacial IL layers (Δ, Figure 3) can be inferred from the oscillation spacing (Figure 2b) or from the average step size in the force profile (Figure 2a and c). For instance, Δ is ~0.75 nm for $[C_2C_1Im][TFSI]$ (*28*), which agrees well with the corresponding ion pair diameter (Ω ~ 0.74 nm) and is consistent with a layered structure composed of cations and anions alike. In contrast, the larger size of the layers for $[C_6C_1Im][TFSI]$ (Δ ~ 1.28 nm) compared to Ω ~ 0.78 nm is attributed to a "bilayer" structure as a result of the higher amphiphilicity of this IL (*29*). The bilayer consists of two $[C_6C_1Im]^+$ cation layers, with the hexyl chains facing each other, and intercalated balancing anions. This is reminiscent of the solvophobic nano-segregation of polar and apolar domains in unconfined (bulk) ILs, which yields a long-range (mesoscopic) continuous sponge-like structure (*30*), highlighting the relation between bulk and interfacial nanostructure. More about the IL nanostructure in the bulk will be described later.

Later studies investigated the influence of confinement and water on the effective viscosity of the nanoconfined ILs (D<5 nm) (*28*, *31*, *32*). IL films with thickness of a few ion pair diameters exhibit an increase in effective viscosity by 1-3 orders of magnitude compared to the bulk IL. This increase depends significantly on the molecular structure of the IL, *e.g.*, ILs with more flexible polyatomic ions, such as those with longer alkyl chains in the cation, are more prone to have higher effective viscosities. These studies revealed that nanoconfined ILs can behave solid-like (in terms of rheology or flow characteristics), which is expected to have implications on the flow behavior of ILs in nanoscopic spaces. It was also shown that water uptake can notably reduce the magnitude of the effective viscosity of the nanoconfined IL films. However, this is out of the scope of this work and will not be further discussed.

Solvation Layers Respond to Applied Surface Potential

The first AFM force measurements that investigated ILs on an electrode surface, Au(111), as a function of applied surface potential were reported by Hayes *et al*. in 2011 (*33*). These studies revealed the number of ion pair layers at the interface increased with the electrode potential, while the innermost layer contracted and became more strongly bound to the surface. This is consistent with the surface-enrichment of counterions that are electrostatically attracted to the electrified surface. This study demonstrated that the surface potential and electrostatic interactions can tune the composition of the interfacial layers. Consistent with this argument, the results also indicated that parameters like ion size, localization of charge, and distance between the electrode and ion can influence the IL interfacial structure, since these parameters influence the strength of the electrostatic interaction. Based on the bulkier molecular structure of the anion $[FAP]^-$ compared to the two investigated cations, force measurements showed that negative potentials (with cations as counterions) led to more ordered interfacial layers compared to negative potentials. The two selected cations were smaller, and exhibit more localized Coulombic charge, and reduced distance from the Au(111) surface charges, compared to $[FAP]^-$. Intermolecular interactions other than electrostatic have been found to also significantly influence the interfacial structure of ILs (*34*, *35*). As an example, imidazolium cations can remain adsorbed on graphene electrodes even at positive bias (*34*, *36*). It thus appears that the subtle balance of electrostatic and non-electrostatic interactions dictates the interfacial composition.

Long-Range Surface Interactions in Highly Concentrated Electrolytes.

The picture that emerged from earlier force measurements was consistent with what was known of a highly concentrated electrolyte, i.e., a collapsed diffuse layer with a Debye length < 1 nm. Force measurements described in previous sections had revealed a solvation force with a short-range oscillating decay profile, suggesting that, at an electrified interface, the charge would be stored within a few ion layers.

In 2013, Israelachvili's group reported the first SFA measurements of a long-range force in $[C_4C_1Im][TFSI]$ (*14*). The decay length of this force was ~ 11 nm, approximately 100x larger than the expected Debye length of the electrolyte, and the sign of the long-ranged force changed with the applied potential to the gold surface, suggesting it was a force arising from overlapping double layers through a diffuse layer. To rationalize these results, it was proposed that the IL behaves as a dilute electrolyte solution, as most of the ions were bound up in a network formed of neutral ion pairs, assumed not to screen the charged surface, with only an extremely small number of free ions, not bound up. Using the obtained screening length and the equation for the Debye screening length of dilute electrolytes, the authors estimated the percentage of free ions to be less than 0.1% within the diffuse layer, which is representative of the bulk composition of the electrolyte according to the Debye-Hückel theory. A subsequent study by the same group (*37*) demonstrated that, as shown in Figure 4, the decay length of the long-range force decreases with increasing temperature, reflecting an increase in the concentration of free ions, supporting the picture of a diffuse double layer and describing the equilibrium between free ions and a network of neutral ion pairs. This long-range force was reported to be modified by the presence of water (Figure 2*c*).

These results came as a surprise to the field, since these long-ranged forces were not measured in earlier SFA/SFB experiments. Moreover, based on contrasting results of short-range vs. long-range surface forces mediated by ILs, Perkin and Israelachvili's groups (*38*, *39*) debated the question whether ILs should behave as "strongly dissociated and, hence, uncorrelated electrolyte" or "as an

effectively neutral, coordinated cation–anion network that exists in equilibrium with a small fraction of effectively dissociated ions" – as quoted in ref. (*39*). The latter implies that only a small fraction of the IL ions contributes to the electrostatic screening of electrified surfaces, "while the majority of the remaining ions behave like neutral aggregates similar to a solvent," as proposed by Gebbie *et al.* (*14*).

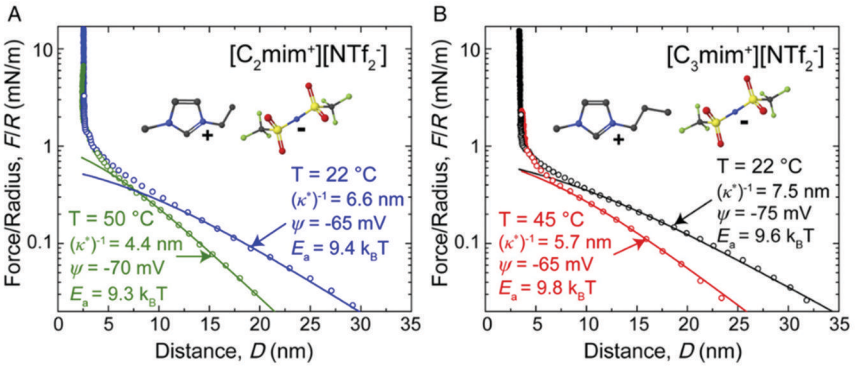

Figure 4. Surface forces across (A) [C_2C_1Im][TFSI] at T = 22 °C and 50 °C and (B) [C_3C_1Im][TFSI] at T = 22 °C and 45 °C, using the nomenclature for ILs in this article. Reproduced with permission from reference (*37*). *Copyright 2015 National Academy of Sciences of the United States of America.*

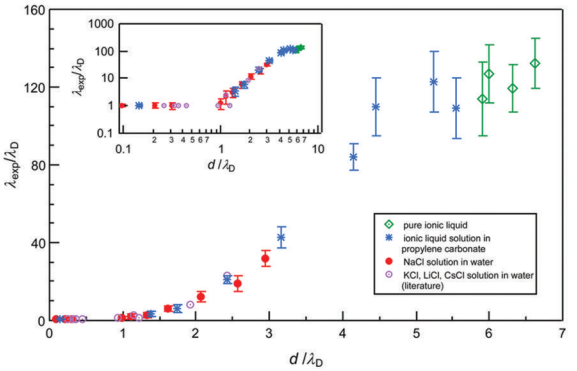

Figure 5. Experimental decay length over the Debye length, λ_{exp}/λ_D, versus d/λ_D for [C_4C_1Pyrr][NTf_2], its mixtures with propylene carbonate, aqueous NaCl, LiCl, KCl, and CsCl solutions. Adapted with permission from reference (*17*). *Copyright 2016 American Chemical Society.*

Subsequent force measurements using a SFB by Perkin's group showed similar long-range forces between mica surfaces for a wide range of highly concentrated electrolytes, including ILs and aqueous salt solutions (*17*). Perkin's group found that the decay length decreases with increasing concentration until ~1 M is reached (in the dilute regime), and then the decay length was found to increase with concentration (in the concentrated regime). Upon plotting the decay length over the theoretically expected Debye length (λ_d) as a function of the "length scale of an ion" (d) over λ_d, it was found that the different electrolytes appeared to collapse onto a single, universal curve.

In the dilute regime, one finds $\frac{\lambda_S}{\lambda_d} = 1$, but the scaling relationship was found as $\frac{\lambda_S}{\lambda_d} \propto \left(\frac{d}{\lambda_d}\right)^3$ in the concentrated regime (Figure 5). The origin of this scaling relationship has been intensively investigated, as outlined in the theory section (*18*).

We note, however, that deviations from this scaling relationship have been reported for both pure ILs and mixtures of ILs and water (*28*, *31*, *40–43*), showing that the decay lengths extracted from the long-range forces do not always fall onto the universal law suggested by Perkin's group. Similarly, comprehensive AFM measurements between smooth silica surfaces using chloride salts of various alkali metals in the range from 1 mM to 5 M, showed no indication of anomalous long range electrostatic forces at temperatures of 25 °C and 45 °C, but instead attractive van der Waals interactions at tip-sample separations of ~2 nm and beyond for salt concentrations of 1 M and higher (*44*).

This calls for alternative analysis and understanding. Moreover, the proposed scaling law requires that the length scale of ions is well known. In the context of ILs, the cation and anion are often of drastically different sizes, and even further, the cation and anion are usually neither symmetric nor have roughly spherical shapes, but their molecular structures are instead, complicated, floppy and oblong. This indicates that there is uncertainty in knowing this parameter for ILs, which is reflected in the spread of the values for neat ILs on this curve. Therefore, amongst other issues discussed in the theory Section, alternative analysis is sought to understand these long-ranged forces.

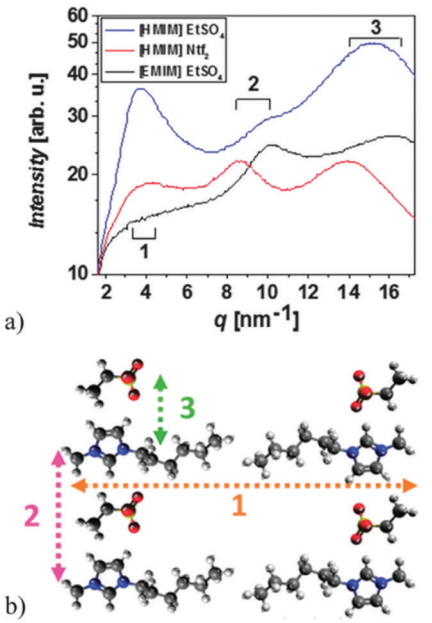

Figure 6. (a) WAXS for dry [C_6C_1Im][$EtSO_4$], [C_6C_1Im][TFSI] and [C_2C_1Im][$EtSO_4$]. (b) Schematic representation of the correlation distances. Reproduced with permission from reference (*40*). *Copyright 2015 Royal Society of Chemistry.*

Ion Aggregation Model

It is well-accepted that IL ions self-assemble in the bulk and can form organized nanostructures (*45*). ILs with $[C_nC_1Im]^+$ cations exhibit three structure factor reflections corresponding to spatial correlation lengths between 3.15 to 0.314 nm (*46*). To illustrate this, Figure 6a shows wide angle x-ray scattering (WAXS) measurements for three different imidazolium ILs (*40*). Hettige *et al*. described the molecular scale origin of these reflections (*46*). The lowest *q* reflection is a description of the average lateral separation between IL filaments or columnar structures of IL bundles (1 in Figure 6a-b) in a disordered continuous network; the mid *q* reflects the longitudinal distance between alkyl tails along a IL filament (2 in Figure 6a-b); and the higher *q* arises due to the average distance between charges within the IL filament (3 in Figure 6a-b). The peak at low *q* in ILs indicates that bulk order can be propagated over relatively large distances (of nanometer size), often in the form of a disordered bicontinuous or sponge-like structure, in which the ions form a network of alternating polar and non-polar domains, presumably due to electrostatic and solvophobic clustering. Both the alkyl chain length and the anion influence the organization of the ions in the bulk, and hence, the nanostructure is more or less significant in different ILs (*40*). The size of these ordered domains is inversely proportional to the full width at half max of the peak at low *q*. As inferred from the width of the first reflection (2.3 and 5.3 $Å^{-1}$ for $[C_6C_1Im][EtSO4]$ and $[C_6C_1Im][TFSI]$ in Figure 6a, respectively), the domain size in $[C_6C_1Im][EtSO4]$ (represented here by columnar bilayer structures, Figure 6b) is twice as large as that obtained for $[C_6C_1Im][TFSI]$, which indicates that the order propagated over larger distances (at the nanoscale) in the former. For readers interested in the bulk nanostructure of ILs, we refer to a comprehensive review by Hayes *et al*. (*47*)

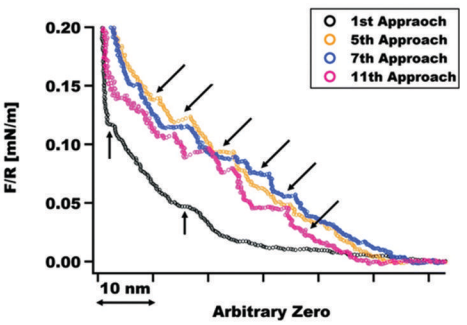

Figure 7. Surface forces measured with a colloidal probe (SiO_2) on mica in dry $[C_6C_1Im][EtSO_4]$ by AFM. The measurements were taken at an offset position of 50 μm from the location of the initial measurement. The results from the 1st, 5th, 7th, and 11th approach of the colloidal probe to mica are shown here. Adapted with permission from reference (40). Copyright 2015. Royal Society of Chemistry.

Restricting ILs to only form ion pairs is unappealing, as in such a concentrated electrolyte, these ion pairs organize to form mesoscopic ionic structures (*48*). If sufficiently strong correlations exist, these larger self-assembled structures could give rise to long-ranged interactions upon compression in a surface force experiment. Consistent with this idea, there has been some evidence of a *longer-range interfacial order in ILs*. Indeed, steps extending to ~60 nm from the surface were observed in the long-range force between mica surfaces (using a SFA) and between mica and a colloidal sphere (by

AFM) in $[C_6C_1Im][EtSO_4]$ (*40*); see Figure 7. The steps varied in size from 0.5 to 3 nm, indicating the presence of ordered domains larger than the size of an ion pair. Interestingly, the surface force increased in range in consecutive force-distance curves, indicating a gradual transition of the behavior of the IL. These ordered domains remained on the surface upon separation, which indicated that the IL might undergo a transition from a disordered/isotropic liquid to a solid or gel (*49*). Uptake of water, on the other hand, was shown to prevent the onset of this liquid-to-solid/gel transition (*41*).

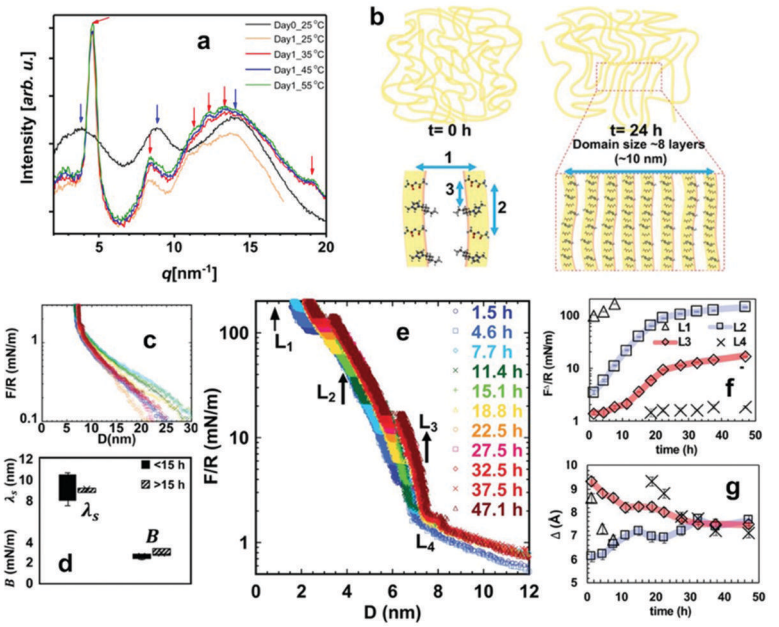

Figure 8. (a) Wide angle X-ray scattering scans of $[C_6C_1Im][TFSI]$ at various temperatures; similar results are obtained for $[C_2C_1Im][EtSO_4]$. (b) Schematics of the domain ordering for $[C_6C_1Im][TFSI]$ postulated based on WAXS. (c) Long-range surface force between mica surfaces in $[C_2C_1Im][EtSO_4]$ over time while equilibrated with dry N_2. (d) Decay length λ_s and constant B after less than and more than 15 h of measurement. (e) Short-range surface force; the legend gives the point of time at D = 100 nm in each force-separation curve. (f) Change of the normalized force (F^{Δ}/R, energy per unit area) required to squeeze out layers L_1, L_2, L_3, and L_4 (g) and of the thickness of the corresponding layers (Δ) over time. Similar results were obtained for $[C_6C_1Im][TFSI]$. Adapted with permission from reference (*50*). *Copyright 2020 John Wiley & Sons, Inc.*

There is also evidence for an ultra-slow transition in common imidazolium ILs (*50*). WAXS experiments revealed that the reflections shown in Figure 6a (taken immediately after filling the X-ray capillary with the IL) changed over time (Figure 8a). Bragg peak and harmonic peaks developed after at most one day incubation of $[C_2C_1Im][EtSO_4]$ and $[C_6C_1Im][TFSI]$. One example is shown in Figure 8a; see that the peak at the lowest q and the red arrows pointing at the harmonics. Other reflections (at mid and high q values) also shift over time, indicating a change of structure. The results pointed at the gradual ordering of the ions in domains of ~10 nm size while adopting a 1D lamellar structure in the bulk (Figure 8b). Over a similar period of time, SFA measurements showed the

evolution of the surface force (Figure 8c-e). Note that if these ordered domains would be affine to the mica/IL interface, they would cause a long-range repulsive force of osmotic nature with a decay length of ~10 nm, which is consistent with the measured long-range force mediated by these ILs. Furthermore, the change of the domain structure inferred from WAXS measurements should cause a change of the short-range structural force, which was also confirmed in SFA force measurements for the investigated ILs (Figure 8e-g). This study thus proposed an alternative explanation for the long-range force based on ion aggregation (*49*).

These findings also enabled to provide an explanation for an apparent discrepancy in the literature. AFM force measurements have typically failed to measure the long-ranged force observed in SFA experiments. This could be justified by the much shorter equilibration times (less than 1 h) required in AFM compared to SFA experiments. Perhaps, this short equilibration time is not sufficient for the ion ordering to happen in the commonly investigated ILs. Interestingly, Rutland's group reported AFM force measurements at temperatures up to 120 °C, which showed the appearance of the long-ranged force for EAN upon an increase in temperature (*51*). This suggests the existence of an Arrhenius-type phase transformation that requires long equilibration times to happen and becomes measurable by AFM at short equilibration times if the temperature is sufficiently high.

Findings from Theory

The structure of the EDL, as inferred from force measurements, has two main features: a short-range structure and a long-range structure. The short-range structure is characterized by strongly bound alternating layers of cations and anions, otherwise known as overscreening. The short-range overscreening structure in concentrated electrolytes has been known for a long time, and theories exist, of various approximations, which can describe this effect. The long-range structure, which is characterized by monotonic and extremely slowly decaying forces, is not well agreed upon, and is still under intensive research.

Overscreening and Short-Range Interactions

In a dilute electrolyte, the charge density surrounding an ion monotonically decays until the charge of the central ion is screened (*52*). This is not always the case, however. There comes a concentration where the decay mode is no longer characterized by real eigenvalues, but instead they become complex, giving rise to decaying oscillations in charge density. This is known as the Kirkwood transition, and has been extensively studied in primitive models of electrolytes. We shall not review this in detail here but point the readers to refs. (*53*, *54*) as our focus is on ILs. Moreover, coarse grained and atomistic simulations of ILs, and other concentrated electrolytes, also find overscreening around central ions in the bulk or as a function of distance from an interface (*15*). For detailed reviews of overscreening, we point readers to refs. (*15*, *55*)

Since Kornyshev's first theory for properties of ILs at interfaces (*56*), which predicted monotonically decaying charge density instead of overscreening (*57*, *58*), there were efforts to develop theories of a similar complexity, but which could capture the overscreening structure of ILs (*15*). In the context of ILs, one of the first theories that was able to achieve this was developed by Bazant, Storey and Kornyshev, otherwise known as the BSK theory (*59*). This theory, with a similar form to a Landau-Ginzburg free energy, was obtained from a gradient expansion of the non-local interaction, giving rise to an additional free energy term. This additional term results in a modified Poisson-Boltzmann equation that contains higher order derivatives:

$$\epsilon(1 - l_c^2\nabla^2\phi)\nabla^2\phi = -\rho$$

Eq. (1)

where ϵ is the dielectric constant, l_c is the correlation length of the electrostatic interactions, and ϕ and ρ are, respectively, the electrostatic potential and charge density. In the regime of linear response, complex roots for the screening length are possible, which indicates the onset of overscreening. In Figure 9, the charge density from the BSK theory is shown for various surface charges. One of the successes of the theory was capturing the transition from overscreening at small potentials to crowding at large potentials, where layers of counterions accumulate, as the charge density was based on a Bikerman excess chemical potential. Interestingly, it has been shown by Avni *et al.* (*60*), a BSK type equation can be derived from considering small ordered ionic clusters, indicating a link between overscreening and ionic associations.

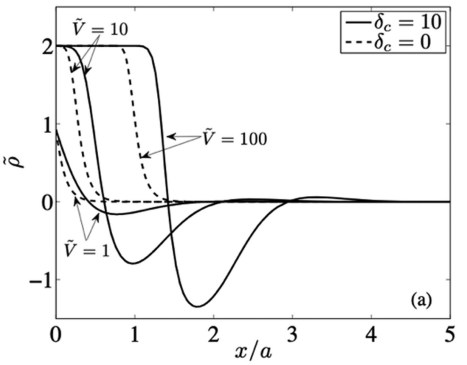

Figure 9. Charge density as a function of distance from the interface, for various surface voltages, and correlation parameters $\delta_c = l_c/\lambda_d$. Reproduced with permission from reference (59). Copyright 2011 American Physical Society.

The BSK theory has been widely employed, but it suffers from two limitations: the period of the oscillation is not fixed by the diameter of an ion, as it must be for layered structures of cations and anions, and the extent of overscreening is not pronounced, as seen in Figure 9, with only one main layer of co-charge being observed. These shortcomings of the theory motivated many to develop theories beyond the BSK theory. Examples of this include a Landau-Ginzburg theory developed by Limmer (*61*), where overscreening is modelled as a phase transition at the interface. Another example is the work by Gavish *et al.* (*62*), which utilized the Cahn-Hilliard phase field terms to describe spinodal decomposition, separating out layers of cations and anions. Conceptually it is required to interpret the Cahn-Hilliard phase field term as arising from van der Waals interactions between like charges, not from electrostatic correlations.

More recently, de Souza *et al.* (*63*) developed a weighted density approximation and applied it to ILs. This method is inspired by Rosenfeld's fundamental measure theory (*64*), where convolutions of weighting functions are used to describe the hard sphere interactions between species. In de Souza and co-worker's theory (*63*), the charge density and electrostatic potential variables, typically taken to be completely local quantities based on point-like ions, are replaced by weighted variables, which are given by the convolution of the variable with a weight function that spreads out the interactions

over the length scale of ions. In linear response, the resulting modified Poisson-Bolztmann equation was found to be:

$$l_D^2 \nabla^2 \phi - (1 + l_c^2 \nabla^2)^2 \phi = 0$$

Eq. (2)

where l_c is now directly proportional to the ion diameter, and the period of the overscreening structure is set by the size of an ion. Moreover, as shown in Figure 10, the theory is able to almost quantitatively describe the overscreening and ionic layering that is observed in molecular dynamics simulations. The theory tends to underestimate the extent of overscreening at large distance, but the overall behavior is very similar.

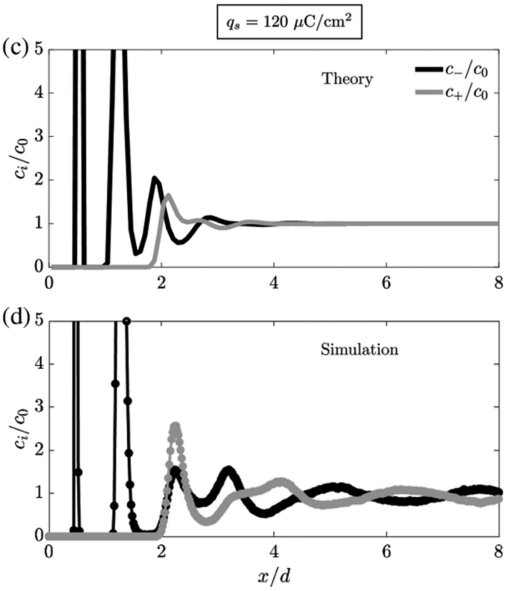

Figure 10. Layering of cations and anions at an interface from theory and simulation. Reproduced with permission from reference (*63*)*. Copyright 2020 American Physical Society.*

Having described briefly the simple theories for overscreening in ILs, we now turn to predictions of short-range surface force interactions. To do this, one needs to calculate the disjoining pressure from the grand potential. In Ref. (*65*), de Souza *et al*. investigated surface force interactions in symmetric and asymmetric ILs using simulations and theory, at various surface charges. Their results are reproduced in Figure 11. For symmetric ILs, there is a strong oscillatory pressure, which arises because of the pronounced layered overscreening structure. Overall, the theory is able to reproduce the features of the simulation extremely well, with the main discrepancy only being the pressure minimum at ~1 nm. For asymmetric ILs, the overscreening structure is less pronounced, but an ion size asymmetric variant of the theory is still able to capture the results extremely well. Overall, the short-range forces from overscreening are well understood from theory, with almost quantitative predictions being possible. For further information, the reader is referred to ref. (*66*).

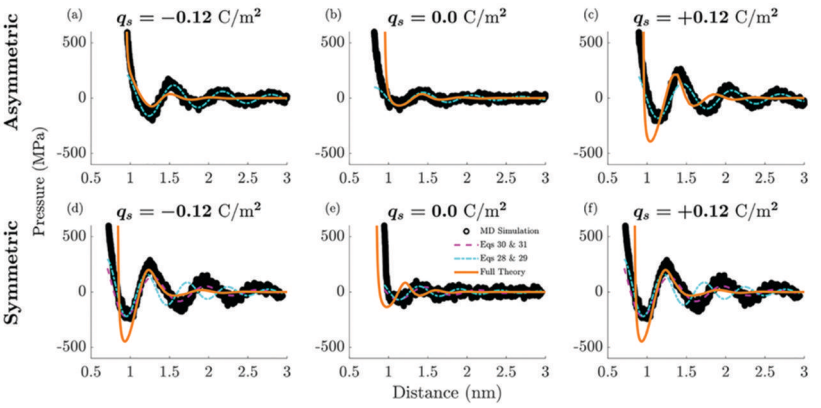

Figure 11. Surface pressure calculated for various surfaces charges, for symmetric and asymmetric ionic liquids. Adapted with permission from reference (65). *Copyright 2022 American Chemical Society.*

Underscreening and Long-Range Interactions

Gebbie *et al*. interpreted their monotonic, long-ranged forces between charged surfaces (Figure 4), as ILs behaving as a "dilute electrolyte", owing to over 99.99% of the ions being bound up into "an effectively neutral, coordinated cation–anion network" (*39*), which are assumed not to contribute to screening of the charged surfaces. While this initial hypothesis was strongly opposed, it motivated many to estimate the extent of ion pairing in ILs, or the number of free ions not bound up into ion pairs, and the role that these ion pairs would have in the EDL.

From a theoretical point of view, Lee *et al*. (*67*) estimated the fraction of free ions to be 2/3 based on a chemical equilibrium between free ions and ion pairs, with an equilibrium constant determined by the McMillan-Mayer theory with the interaction potential based on the Debye-Hückel screened interaction in the IL. As the Debye-Hückel screening length (λ_d) is much smaller than an ion diameter in ILs (d), the ions effectively did not interact, and the entropy of mixing decided the proportion of each species. A more phenomenological approach was taken by Chen *et al*. (*68*), where the association constant of the equilibrium between free ions and ion pairs was assumed to be a parameter of the theory. This parameter was estimated from fitting the temperature dependence of the differential capacitance (the derivative of surface charge with respect to electrode potential drop, or more precisely, the rate of change of the stored charge divided by the rate of change of the surface potential) obtained from MD simulations. It was estimated that between 30-40 % of ions were free, depending on the temperature.

In a different approach, Ma *et al*. (*69*) developed a sophisticated classical density functional theory approach of free ions and ion pairs, where the equilibrium between them can be set. Ma *et al*. also studied the EDL structure and surface forces. This was done with no ion pairs and various degrees of ion pairing. The short-range structure of the EDL between these two extreme cases were very similar, which can actually be understood from earlier work on the similarities between the phase diagram of ionic fluids and dipolar fluids, as reviewed in ref. (*70*). Their calculations found monotonic long-ranged forces existed for over 99% of ions being free, but not for 0% and 95%, as shown in Figure 12a. However, the calculated differential capacitance curves for these cases were drastically different close to the potential of zero charge. For 99.9% of ions paired, there was a substantial U-shape, but for 0% of ion pairs, a bell-shaped differential capacitance curve was found.

These calculations provided insight into the EDL with many ion pairs, but unfortunately, not all aspects of the EDL were able to be reconciled. These results inspired Goodwin and Kornyshev (*71*) to demonstrate that the capacitance could, in fact, have reasonable values despite corresponding to over 99.99% paired ions, in a model of the charge density with two decay lengths – one overscreening with short decay length and another monotonic decay length with a larger length scale. Provided the magnitude of the monotonic decaying contribution is small, and the majority of the electrode charge is screened by the short-range overscreening part, non-vanishing capacitance values could be obtained, despite the long tail of the charge density. This has yet to be realized in simulations of ILs, however.

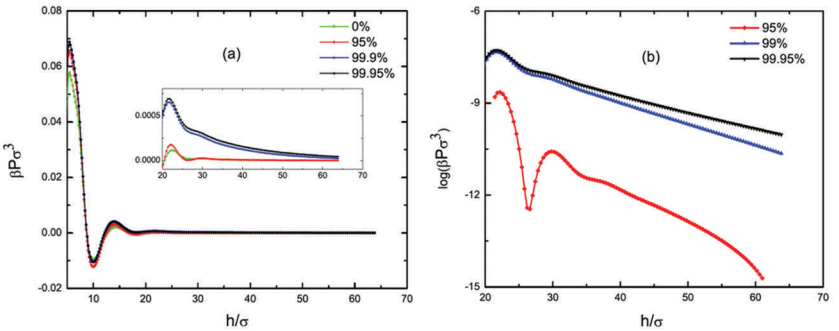

Figure 12. Surface pressure calculated between like-charged interfaces, for various extents of ion pairing. Reproduced with permission from reference (*69*)*. Copyright 2015 AIP Publishing.*

Moreover, not only is the massive extent of ion pairing at odds with the differential capacitance, but also the electrical conductivity of ILs, which is typically only found to slightly deviate from that expected from the Nernst-Einstein equation. A notable example comes from Feng *et al.* (*72*), where a dynamical criterion was utilized to estimate that between 15-30% of ions were free depending on the temperature. Moreover, the dynamical criterion was tested against more conventional separation-based methods, and good agreement was found. This permitted the temperature dependence of the electrical conductivity to be well reproduced, which is usually offset from the ideal line on the Walden plot, which has been interpreted as ILs forming ion pairs.

In this "underscreening regime", the proposed name of these long-ranged interactions, the screening length λ_s scaled as $\frac{\lambda_s}{\lambda_d} \propto \left(\frac{d}{\lambda_d}\right)^3$, where d is ion diameter (*17*). It was proposed by Lee *et al.* (*73*) that in the underscreening regime of concentrated electrolytes, the charge carrier is no longer the ions, but either the solvent molecules, voids, or the neutral alkly chains in ILs. This concept is similar to the conduction of holes in semiconductors, or the conduction of vacancies in solid electrolytes (*15*). While the scaling relationship observed in experiments was recovered, the proposal of ions no longer carrying charge in ILs has not been widely adopted, and alternative explanations are still sought.

There have been many examples of restricted primitive models of electrolytes being studied, to see if long-ranged monotonic screening lengths can be found. Overall, it has always been found that, after the Kirkwood transition, the screening length increases with concentration, but the power law dependence of Smith *et al.* (*17*) has not yet been found (Figure 5). Instead of an exponent of 3, an exponent of 2 or smaller is often obtained. Moreover, the magnitude of the screening length is often

significantly smaller than found in the experiments discussed in previous sections. In experiments, the observed screening length is up to 100x that of the Debye length (Figures 4-8), but from theory it typically only reaches 5x (*74*, *75*). Therefore, it does not appear that the screening length observed can be understood from electrostatic correlations in primitive models.

To name some examples, Coupette *et al*. (*76*) found screening lengths up to 0.5 nm, and that multiple decay lengths could exist, but did not find the scaling relationship of Smith *et al*. (*17*) Another example comes from de Souza's (*63*) weighted density approximation, where the screening length ($1/\kappa_s$) was found to be

$$\kappa_s \lambda_d = \frac{1 \pm \sqrt{1 - 4\left(\frac{l_s}{\lambda_d}\right)^2}}{2\left(\frac{l_s}{\lambda_d}\right)^2}$$

Eq. (3)

where $l_s = d/\sqrt{24}$. This means the screening length over the Debye length scales as $\sim \left(\frac{d}{\lambda_s}\right)^2$ for a concentrated electrolyte, such as an IL. Similarly, Adar *et al*. obtained a similar relationship (*74*). Large scale MD simulations by Krucker-Velasquez and Swan (*77*), and Zeeman *et al*. (*78*) did not find screening lengths or the scaling proposed by Smith *et al.* (*17*), with them always finding exponents close to 2, with much smaller magnitudes for the screening length than found in experiments.

Thus far, then, the conceptually simple ion pairing model, typically used to understand the experiments of Gebbie *et al*. (*14*, *37*), and primitive model approaches don't appear to be able to explain these long-ranged interactions. In a concentrated system, however, one would not just expect ion pairs to form. Larger aggregates of ions should form as a consequence of their close proximity. Such large clusters have been reported in MD simulations (*45*, *49*, *79*), and even aggregates that percolate throughout the whole simulation box. There is relatively little work on the role of aggregates in concentrated electrolytes, however, but it appears to be an area that is being further explored now.

McEldrew *et al*. (*45*, *49*, *79*) recently developed a theory for aggregation and gelation (formation of a percolating ionic network) in concentrated electrolytes, based on the classical polymer theories of thermoreversible aggregation by Flory, Stockamyer and Tanaka. This theory of McEldrew *et al*. is a consistent treatment of ionic associations, which can be used to calculate a wide variety of properties of electrolytes, such as transference numbers, activity coefficients, and more recently, also EDL properties. In the context of the EDL, Goodwin *et al*. developed an approach to treat aggregates in the EDL of ILs, based on a Boltzmann closure relation for the cluster distribution (*80*, *81*). This theory demonstrated that aggregates and a percolating ionic network, could in fact, contribute to ionic screening. In previous studies, it was usually simply assumed that any aggregates act as neutral ion pairs which cannot contribute to screening. However, Goodwin *et al*. (*81*) showed, from the reversible nature of the associations, that charged aggregates and a *gel* (ionic network) form in the EDL, owing to the unequal numbers of cations and anions, which can screen electrode charge. Therefore, it appears that the assumption of the "network of neutral ion pairs" not contributing to screening electrode charge is not correct, owing to the thermo-reversible nature of the ionic associations. Moreover, owing to the screening ability of the gel and aggregates, to obtain the screening lengths of Gebbie *et al.* (*14*) and Smith *et al.* (*17*), even smaller free ion fractions are

required. These results suggest that, while ionic aggregation occurs in ILs, the origin of the long-ranged forces cannot solely be attributed to charge renormalisation in ILs. This is consistent with the experimental findings by Han *et al*. (Figure 8) (*50*), which showed the association of the IL ions in domains as large as 10 nm, and correlated this network with short- and long-range force between negatively charged surfaces.

Discussion

As described in the previous sections, the theoretical concept of long-range screening (or underscreening) in ILs cannot explain all experimental observations, which indicates that the current knowledge of the EDL structure of ILs, and more broadly, of highly concentrated electrolytes, is only partial. There is clear evidence that emphasizes the need of alternative models and calls for further investigation. This includes the EDL capacitance of ILs, where capacitance characterizes the amount of charge stored in the EDL and is generally voltage-dependent. In the pioneering theory of Kornyshev for ILs (*56*), it was demonstrated that the differential capacitance of ILs exhibits either a 'camel' or a 'bell' shape, instead of the classical U-shape based on Gouy-Chapman theory (*15*). Both experiments and molecular simulations find, indeed, either bell or camel-shaped differential capacitance curves for ILs (Figure 13a). In Kornyshev's theory, the camel-to-bell transition occurred when over 1/3 of the volume was occupied by ions. In ILs, however, it is well known that over 95% of the space is occupied by ions. To rationalize this observation, either the orientation of ions can be invoked or the compacity parameter can be re-interpreted as the fraction of free ions, where the "voids" represent neutral ion pairs (*68*). In the latter case, the differential capacitance curve will transition from a camel to a bell shape with increasing temperature, provided the number of free ions goes over 1/3 (according to ref. (*68*)) or ½ in Goodwin-Kornyshev's more recent ion pairing model (*80*).

Typically, the magnitude of the IL differential capacitance is in the range of 5-25 μF cm^{-2}, with either a camel or bell-like shape (*15*). If one would assume the extent of ion pairing suggested by Gebbie *et al*., extremely small capacitance values would be obtained and a strong U-shaped differential capacitance curve would be found (*71*). Therefore, it appears that interpreting the decay length from the surface force measurements as extreme ion pairing is inconsistent with differential capacitance measurements.

Moreover, the conductivity of ILs is often found to only slightly deviate from what is expected from the Nernst-Einstein equation of the uncorrelated ions (*72*). This has been interpreted as some percentage of the ions bound up in ion pairs, with this simple assumption estimates the fraction of free ions at 0.1-0.2, depending on the temperature. Therefore, the concentration of charge carriers from conductivity measurements also appears to be much larger than that suggested by surface force measurements when interpreted in the context of dilute electrolytes.

Finally, studies of stability of particle dispersions in pure ILs and in mixtures of ILs and water are not consistent with a long-range electrostatic repulsion between particles. These studies have shown that the mechanisms underlying particle stability and aggregation are very different in diluted and concentrated ILs (*82–85*). Indeed, the DLVO theory describes well the behavior of particle dispersions in diluted ILs, and hence, electrostatic interactions mainly determine particle stability in this regime (*85*). In contrast, viscous and solvation forces explain particle stability in concentrated and pure ILs, and no evidence was found for the action of a long-range electrostatic repulsion between the particles (*82–85*). Viscous stabilization results from the slow diffusion of particles in viscous (concentrated) ILs, while solvation stabilization is due to the interfacial layering of ILs. It

has been also reported that ion specificity can play an important role in the adsorption process, and thereby in particle stability (*86*).

In light of the results reviewed in the theory Section, it appears that alternative explanations to the origin of the slowly decaying surface forces should be entertained. The theoretical results suggest the experimental obtained decay length does not originate from electrostatic screening alone, otherwise it would be captured by the primitive models. Moreover, theory indicates the extent of ions which appear to be free, not bound in ion pairs or aggregates, is of the order of 10%, rather than 0.003%, as suggested by Gebbie *et al*. In the experimental Section, we summarized a possible alternative explanation, based on ionic aggregates giving rise to long-ranged forces with slow dynamics. In fact, in certain highly concentrated electrolytes (*42*), the force profile appears more logarithmic than exponential, which could suggest the osmotic origin of the force. Overall, if the origin of these forces is not purely electrostatic screening related, one could be able to reconcile capacitance and conductivity measurements with these experiments.

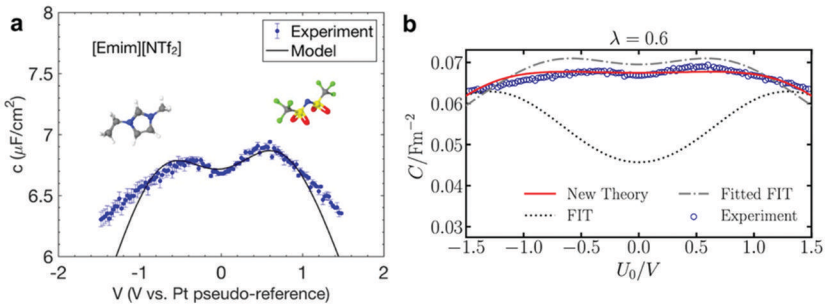

Figure 13. (a) Differential capacitance of [C_2C_1Im][TFSI] with the markers representing the experiment and the solid lines corresponding to the fit of the extended mean-field model to experimental results. Reproduced with permission from reference (*87*)*. Copyright 2018 American Chemical Society. (b) The new theory by Goodwin et al. is in better agreement with the experimental differential capacitance than the free ion theory (FIT). Reproduced with permission from reference* (*81*)*. Copyright 2022 AIP Publishing.*

This can be further demonstrated by Goodwin *et al*.'s recent application of the aggregation theory to the EDL (*81*). They used their theory to reproduce the experimentally obtained differential capacitance curve of [C_2C_1Im][TFSI] from Jitvisate and Seddon (Figure 13a) (*87*). To reproduce the slight camel shape of the curve (Figure 13b), an association constant of ~0.6 needed to be employed. This is well above the percolation point (1/9 for a symmetric functionality of 4), and therefore, it indicates that a gel exists, which is understood as an ionic cluster, and it extends throughout the entire electrolyte. Despite the presence of the gel, the fraction of free ions was 0.12 (12%), which is close to the estimate of Feng *et al.* (*72*) for the conductivity. In addition, charged ionic clusters and gel formed under an applied potential can screen surface charge. Therefore, if the percolating ionic network and charged ionic clusters gives rise to some long-range, osmotic force, whilst still having the correct differential capacitance response and conductivity, all measurements can be unified under the concept of ion aggregation.

ILs are a conceptually simple electrolyte, but the correlations between species are actually not very strong, and the ionic aggregation is typically relatively weak (*45*); although the results described for [C_6C_1Im][$EtSO_4$] (Figure 7) suggest that they could be high enough in some ILs. However, there

are many other highly concentrated electrolytes which are more strongly correlated, one example of which is water-in-salt electrolytes (WiSEs), which combine Li^+ cations with IL anions and small amounts of water (*88*). The aggregation behavior of these electrolytes is significantly more pronounced (*89*).

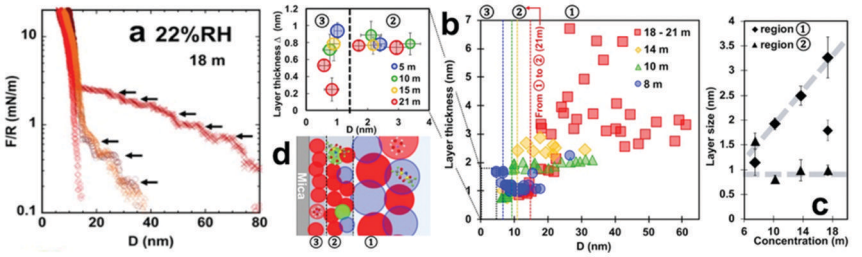

Figure 14. (a) Surface forces in LiTFSI 18m in water between mica surfaces measured by eSFA. (b) Layer size vs. separation between the mica surfaces. The inset shows the size of the layers at separations smaller than 4 nm. (c) Layer thickness as a function of the concentration of LiTFSI in water. (d) Cartoon of the interfacial structure of superconcentrated LiTFSI in water. There are three different regions based on the interfacial layers inferred from short-range and long-range forces. Adapted with permission from reference (42). Copyright 2021 American Chemical Society.

In this context, SFA force measurements by Han *et al*. (*42*) have shown long-range surface forces in WiSEs, specifically LiTFSI at concentrations ranging between 8 and 21 m in water. The long-range force is detected at surface separations as large as ~88 nm, but it is not exponentially decaying (Figure 14a). The profile of the long-range force appears reminiscent of a polymer- or polyelectrolyte-induced repulsion. The force-distance curves also have superposed steps, as layers are squeezed-out. The size of the structural units forming these layers increases monotonically with concentration (Δ_1 = 1.0−6.0 nm) between 8 and 21 m (Figure 14b and inset, and Figure 12c). Separate MD simulations and small angle scattering measurements have also revealed the formation of nanostructured domains in 21m LiTFSI in water (*90*). Below a concentration of 8 m, the long-range nanostructure of the bulk electrolyte vanishes, as also the long-range force disappears, indicating the direct relation between the electrolyte nanostructure and the origin of this long-range force. In the range of concentrations 9-21m, the size of the structural unit (charged ionic clusters) decreases closer to the surface (Δ_2 ~ 0.80−0.99 nm, Figure 14c), independently of concentration, reflecting that the nanostructure is significantly disturbed by the presence of the charged and hydrophilic surface. Originating from the negative charge of the mica surface, the innermost layer (Δ_3) is most likely rich in Li+ and water (Figure 14b inset). The conceptual model of this short- and long-range structure of the EDL is shown in Figure 14d.

The differential capacitance of 21m LiTFSI in water on gold was also determined and compared to that of 1 m LiTFSI (dilute electrolyte) (*91*) Figure 15 compares the results from these measurements. Combining AFM force measurements and vibrational spectroscopy, the short-range structure of the highly concentrated electrolyte was investigated as a function of the applied potential, to complement the conceptual picture shown in Figure 14d. Two layers of $[Li(H2O)x]^+$ (2.8 and 3.3 Å, respectively) were found at negative potentials, consistent with the findings in Figure 14b (region 3) for negatively charged mica. On the other hand, thicker layers (6.4 and 6.7 Å) composed of

[Li(H2O)x]+([TFSI]−)y clusters were detected only at the interface with gold at positive potentials, and hence, it was inferred that they carry a negative charge. These clusters were not resolved in the dilute electrolyte. Overall, the differential capacitance of this highly concentrated electrolyte was found to be ~50% larger than that of the dilute solution (1m LiTFSI). Furthermore, ultramicroelectrode measurements revealed the layered structure imposes a confinement effect on ferricyanide redox couple at the electrode/WiSE interface, which hinders diffusion. Such nanostructure may be also key in determining redox reactions, and hence, can have other practical implications.

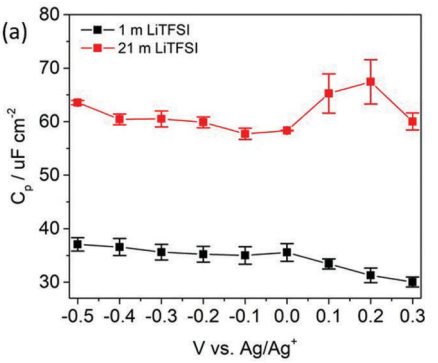

Figure 15. Differential capacitance of 1 m and 21m LiTFSI aqueous solutions on gold Au(111). Adapted with permission from reference (91). Copyright 2020 American Chemical Society.

Conclusions

This chapter has reviewed measurements of colloidal forces mediated by ILs and theoretical findings describing their origin (*92*). Surface forces in ILs include two main components— short-range (structural) forces and long-range forces with a slow decay. Both SFA and AFM measurements have shown that the short-range interaction has an oscillatory nature, with the spacing of the oscillation corresponding to the dimension of an ion pair. This indicates the arrangement of the IL ions in layers close to the solid surface. Numerous experiments have shown that the interfacial layers of ILs can be tuned by water uptake, surface composition, potential/charge, ion size and charge localization, among others. Theory has been able to describe ionic layering as a result of overscreening of the surface charge, and also to reproduce (almost quantitatively) the experimentally observed short-range surface forces. The long-range force in ILs was initially interpreted as the electrical double layer force of an effectively dilute electrolyte. It was assumed that most of the ions are bound up in ion pairs and only an extremely small number of ions remain dissociated and able to screen surface charge. However, the proposed charge renormalization is inconsistent with several experimental results, such as differential capacitance and conductivity.

Experiments and theory have also provided an alternative explanation for the large decay length of the long-range force in ILs. Here, a large number of ions remain dissociated and can readily contribute to conductivity, while most of the ILs ions form large ion aggregates and an ionic network that percolates through the IL that can, in fact, also participate in charge screening. This ion aggregation theory can reproduce capacitance curves of ILs and conductivity, and the short-range and long-range structural forces. Experiments suggest that after the distortion of this network, it

requires time (hours) for this ion organization to be recovered in the bulk, which has presumably limited the observation of this force in AFM force measurements. The surface disturbs the ionic network (yielding interfacial layers with size equal to ion pairs) but some experimental methods are sensitive enough to resolve the ionic clusters located further from the surface, especially for other electrolyte systems with stronger ionic correlation, like LiTFSI 21m in water.

Long-range interactions mediated by IL are still under intensive research. The knowledge inferred from these studies is beneficial for applications of ILs as electrolytes in supercapacitors and as lubricants, industrial colloidal systems, as well as in the field of water-in-salt electrolytes and non-aqueous electrolytes for batteries.

Acknowledgments

This material is based upon work supported by the National Science Foundation under Grant DMR-1904681, and CBET 19-16609.

References

1. Welton, T. Room-Temperature Ionic Liquids. Solvents for Synthesis and Catalysis. *Chem. Rev.* **1999**, *99* (8), 2071–2084.
2. Weingartner, H. Understanding ionic liquids at the molecular level: facts, problems, and controversies. *Angew. Chem., Int. Ed. Engl.* **2008**, *47* (4), 654–670.
3. Hallett, J. P.; Welton, T. Room-temperature ionic liquids: solvents for synthesis and catalysis. 2. *Chem. Rev.* **2011**, *111* (5), 3508–3576.
4. Armand, M.; Endres, F.; MacFarlane, D. R.; Ohno, H.; Scrosati, B. Ionic-liquid materials for the electrochemical challenges of the future. *Nat. Mater.* **2009**, *8* (8), 621–629.
5. MacFarlane, D. R.; Tachikawa, N.; Forsyth, M.; Pringle, J. M.; Howlett, P. C.; Elliott, G. D.; Davis, J. H.; Watanabe, M.; Simon, P.; Angell, C. A. Energy applications of ionic liquids. *Energy Environ. Sci.* **2014**, *7* (1), 232–250.
6. Hayes, R.; Warr, G. G.; Atkin, R. At the interface: solvation and designing ionic liquids. *Phys. Chem. Chem. Phys.* **2010**, *12* (8), 1709–1723.
7. Hayes, R.; Wakeham, D.; Atkin, R. Interfaces of Ionic Liquids (2). *Ionic Liq. Uncoiled: Critical Expert Overviews*; John Wiley & Sons, Inc., 2012; pp 51−85.
8. Espinosa-Marzal, R.; Han, M.; Arcifa, A.; Spencer, N.; Rossi, A., Ionic liquids at interfaces and their tribological behavior. *Encyclopedia of Interfacial Chemistry: Surface Science and Electrochemistry*; Elsevier, 2018; pp 172−194.
9. Parvulescu, V. I.; Hardacre, C. Catalysis in ionic liquids. *Chem. Rev.* **2007**, *107* (6), 2615–2665.
10. Cosgrove, T. *Colloid Science: principles, methods and applications*; John Wiley & Sons, 2010.
11. Horn, R. G.; Evans, D. F.; Ninham, B. W. Double-layer and solvation forces measured in a molten salt and its mixtures with water. *J. Phys. Chem.* **1988**, *92* (12), 3531–3537.
12. Atkin, R.; Warr, G. G. Structure in Confined Room-Temperature Ionic Liquids. *J. Phys. Chem. C* **2007**, *111* (13), 5162–5168.
13. Mezger, M.; Schroder, H.; Reichert, H.; Schramm, S.; Okasinski, J. S.; Schoder, S.; Honkimaki, V.; Deutsch, M.; Ocko, B. M.; Ralston, J.; Rohwerder, M.; Stratmann, M.;

Dosch, H. Molecular layering of fluorinated ionic liquids at a charged sapphire (0001) surface. *Science* **2008**, *322* (5900), 424–428.
14. Gebbie, M. A.; Valtiner, M.; Banquy, X.; Fox, E. T.; Henderson, W. A.; Israelachvili, J. N. Ionic liquids behave as dilute electrolyte solutions. *Proc. Natl. Acad. Sci. U. S. A.* **2013**, *110* (24), 9674–9679.
15. Fedorov, M. V.; Kornyshev, A. A. Ionic liquids at electrified interfaces. *Chem. Rev.* **2014**, *114* (5), 2978–3036.
16. Gebbie, M. A.; Smith, A. M.; Dobbs, H. A.; Lee, A. A.; Warr, G. G.; Banquy, X.; Valtiner, M.; Rutland, M. W.; Israelachvili, J. N.; Perkin, S.; Atkin, R. Long range electrostatic forces in ionic liquids. *Chem. Commun. (Cambridge, U. K.)* **2017**, *53* (7), 1214–1224.
17. Smith, A. M.; Lee, A. A.; Perkin, S. The Electrostatic Screening Length in Concentrated Electrolytes Increases with Concentration. *J. Phys. Chem. Lett.* **2016**, *7* (12), 2157–2163.
18. Lee, A. A.; Perez-Martinez, C. S.; Smith, A. M.; Perkin, S. Scaling Analysis of the Screening Length in Concentrated Electrolytes. *Phys. Rev. Lett.* **2017**, *119* (2), 026002.
19. Israelachvili, J. N. *Intermolecular and Surface Forces: Revised Third Edition*; Academic Press, 2011.
20. Pashley, R. DLVO and hydration forces between mica surfaces in Li+, Na+, K+, and Cs+ electrolyte solutions: A correlation of double-layer and hydration forces with surface cation exchange properties. *J. Colloid Interface Sci.* **1981**, *83* (2), 531–546.
21. Miklavic, S. J.; Ninham, B. W. Competitiion for adsorption sites by hydrated ions. *J. Colloid Interface Sci.* **1990**, *134* (2), 305–311.
22. Perkin, S.; Albrecht, T.; Klein, J. Layering and shear properties of an ionic liquid, 1-ethyl-3-methylimidazolium ethylsulfate, confined to nano-films between mica surfaces. *Phys. Chem. Chem. Phys.* **2010**, *12* (6), 1243–1247.
23. Espinosa-Marzal, R. M.; Arcifa, A.; Rossi, A.; Spencer, N. D. Microslips to "Avalanches" in Confined, Molecular Layers of Ionic Liquids. *J. Phys. Chem. Lett.* **2014**, *5* (1), 179–184.
24. Klein, J.; Perahia, D.; Warburg, S. Forces between polymer-bearing surfaces undergoing shear. *Nature* **1991**, *352* (6331), 143–145.
25. Israelachvili, J.; Min, Y.; Akbulut, M.; Alig, A.; Carver, G.; Greene, W.; Kristiansen, K.; Meyer, E.; Pesika, N.; Rosenberg, K. Recent advances in the surface forces apparatus (SFA) technique. *Rep. Prog. Phys.* **2010**, *73* (3), 036601.
26. Espinosa-Marzal, R. M.; Arcifa, A.; Rossi, A.; Spencer, N. D. Ionic Liquids Confined in Hydrophilic Nanocontacts: Structure and Lubricity in the Presence of Water. *J. Phys. Chem. C* **2014**, *118* (12), 6491–6503.
27. Heuberger, M. The extended surface forces apparatus. Part I. Fast spectral correlation interferometry. *Rev. Sci. Instrum.* **2001**, *72* (3), 1700–1707.
28. Han, M.; Espinosa-Marzal, R. M. Electroviscous Retardation of the Squeeze Out of Nanoconfined Ionic Liquids. *J. Phys. Chem. C* **2018**, *122* (37), 21344–21355.
29. Smith, A. M.; Lovelock, K. R.; Perkin, S. Monolayer and bilayer structures in ionic liquids and their mixtures confined to nano-films. *Faraday Discuss.* **2013**, *167* (0), 279–292.
30. Triolo, A.; Russina, O.; Bleif, H. J.; Di Cola, E. Nanoscale segregation in room temperature ionic liquids. *J. Phys. Chem. B* **2007**, *111* (18), 4641–4644.
31. Han, M.; Espinosa-Marzal, R. M. Influence of Water on Structure, Dynamics, and Electrostatics of Hydrophilic and Hydrophobic Ionic Liquids in Charged and Hydrophilic

Confinement between Mica Surfaces. *ACS Appl. Mater. Interfaces* **2019**, *11* (36), 33465–33477.

32. Han, M.; Rogers, S. A.; Espinosa-Marzal, R. M. Rheological Characteristics of Ionic Liquids under Nanoconfinement. *Langmuir* **2022**, *38* (9), 2961–2971.
33. Hayes, R.; Borisenko, N.; Tam, M. K.; Howlett, P. C.; Endres, F.; Atkin, R. Double Layer Structure of Ionic Liquids at the Au(111) Electrode Interface: An Atomic Force Microscopy Investigation. *J. Phys. Chem. C* **2011**, *115* (14), 6855–6863.
34. Fedorov, M. V.; Lynden-Bell, R. M. Probing the neutral graphene-ionic liquid interface: insights from molecular dynamics simulations. *Phys. Chem. Chem. Phys.* **2012**, *14* (8), 2552–2556.
35. He, Z.; Alexandridis, P. Nanoparticles in ionic liquids: interactions and organization. *Phys. Chem. Chem. Phys.* **2015**, *17* (28), 18238–18261.
36. Jurado, L. A.; Espinosa-Marzal, R. M. Insight into the Electrical Double Layer of an Ionic Liquid on Graphene. *Sci. Rep.* **2017**, *7* (1), 4225.
37. Gebbie, M. A.; Dobbs, H. A.; Valtiner, M.; Israelachvili, J. N. Long-range electrostatic screening in ionic liquids. *Proc. Natl. Acad. Sci. U. S. A.* **2015**, *112* (24), 7432–7437.
38. Perkin, S.; Salanne, M.; Madden, P.; Lynden-Bell, R. Is a Stern and diffuse layer model appropriate to ionic liquids at surfaces? *Proc. Natl. Acad. Sci. U. S. A.* **2013**, *110* (44), E4121–E4121.
39. Gebbiea, M. A.; Valtiner, M.; Banquy, X.; Henderson, W. A.; Israelachvili, J. N. Reply to Perkin et al.: Experimental observations demonstrate that ionic liquids form both bound (Stern) and diffuse electric double layers. *Proc. Natl. Acad. Sci. U. S. A.* **2013**, *110* (44), E4122.
40. Jurado, L. A.; Kim, H.; Arcifa, A.; Rossi, A.; Leal, C.; Spencer, N. D.; Espinosa-Marzal, R. M. Irreversible structural change of a dry ionic liquid under nanoconfinement. *Phys. Chem. Chem. Phys.* **2015**, *17* (20), 13613–13624.
41. Jurado, L. A.; Kim, H.; Rossi, A.; Arcifa, A.; Schuh, J. K.; Spencer, N. D.; Leal, C.; Ewoldt, R. H.; Espinosa-Marzal, R. M. Effect of the environmental humidity on the bulk, interfacial and nanoconfined properties of an ionic liquid. *Phys. Chem. Chem. Phys.* **2016**, *18* (32), 22719–22730.
42. Han, M.; Zhang, R.; Gewirth, A. A.; Espinosa-Marzal, R. M. Nanoheterogeneity of LiTFSI Solutions Transitions Close to a Surface and with Concentration. *Nano Lett.* **2021**, *21* (5), 2304–2309.
43. Cheng, H.-W.; Stock, P.; Moeremans, B.; Baimpos, T.; Banquy, X.; Renner, F. U.; Valtiner, M. Characterizing the Influence of Water on Charging and Layering at Electrified Ionic-Liquid/Solid Interfaces. *Adv. Mater. Interfaces* **2015**, *2* (12), 1500159.
44. Kumar, S.; Cats, P.; Alotaibi, M. B.; Ayirala, S. C.; Yousef, A. A.; van Roij, R.; Siretanu, I.; Mugele, F. Absence of anomalous underscreening in highly concentrated aqueous electrolytes confined between smooth silica surfaces. *J. Colloid Interface Sci.* **2022**, *622*, 819–827.
45. McEldrew, M.; Goodwin, Z. A. H.; Zhao, H.; Bazant, M. Z.; Kornyshev, A. A. Correlated Ion Transport and the Gel Phase in Room Temperature Ionic Liquids. *J. Phys. Chem. B* **2021**, *125* (10), 2677–2689.
46. Hettige, J. J.; Araque, J. C.; Margulis, C. J. Bicontinuity and multiple length scale ordering in triphilic hydrogen-bonding ionic liquids. *J. Phys. Chem. B* **2014**, *118* (44), 12706–12716.

47. Hayes, R.; Warr, G. G.; Atkin, R. Structure and nanostructure in ionic liquids. *Chem. Rev.* **2015**, *115* (13), 6357–6426.
48. Russina, O.; Triolo, A.; Gontrani, L.; Caminiti, R. Mesoscopic structural heterogeneities in room-temperature ionic liquids. *J. Phys. Chem. Lett.* **2012**, *3* (1), 27–33.
49. McEldrew, M.; Goodwin, Z. A. H.; Bi, S.; Bazant, M. Z.; Kornyshev, A. A. Theory of ion aggregation and gelation in super-concentrated electrolytes. *J. Chem. Phys.* **2020**, *152* (23), 234506.
50. Han, M.; Kim, H.; Leal, C.; Negrito, M.; Batteas, J. D.; Espinosa-Marzal, R. M. Insight into the Electrical Double Layer of Ionic Liquids Revealed through Its Temporal Evolution. *Adv. Mater. Interfaces* **2020**, *7* (24), 2001313.
51. Hjalmarsson, N.; Atkin, R.; Rutland, M. W. Switchable long-range double layer force observed in a protic ionic liquid. *Chem. Commun. (Cambridge, U. K.)* **2017**, *53* (3), 647–650.
52. Bazant, M. Z.; Kilic, M. S.; Storey, B. D.; Ajdari, A. Towards an understanding of induced-charge electrokinetics at large applied voltages in concentrated solutions. *Adv. Colloid Interface Sci.* **2009**, *152* (1−2), 48–88.
53. Kirkwood, J. G. Statistical Mechanics of Liquid Solutions. *Chem. Rev.* **2002**, *19* (3), 275–307.
54. Attard, P. Electrolytes and the Electric Double Layer. In *Advances in Chemical Physics*; John Wiley & Sons, Ltd, 1996; pp 1–159.
55. Goodwin, Z. A. H.; de Souza, J. P.; Bazant, M. Z.; Kornyshev, A. A. Mean-Field Theory of the Electrical Double Layer in Ionic Liquids. In *Encyclopedia of Ionic Liquids*; Zhang, S., Ed.; Springer Singapore: Singapore, 2021; pp 1−13.
56. Kornyshev, A. A. Double-layer in ionic liquids: paradigm change? *J. Phys. Chem. B* **2007**, *111* (20), 5545–5557.
57. Kilic, M. S.; Bazant, M. Z.; Ajdari, A. Steric effects in the dynamics of electrolytes at large applied voltages. I. Double-layer charging. *Phys. Rev. E: Stat. Nonlin. Soft Matter Phys.* **2007**, *75* (2 Pt 1), 021502.
58. Goodwin, Z. A. H.; Feng, G.; Kornyshev, A. A. Mean-Field Theory of Electrical Double Layer In Ionic Liquids with Account of Short-Range Correlations. *Electrochim. Acta* **2017**, *225*, 190–197.
59. Bazant, M. Z.; Storey, B. D.; Kornyshev, A. A. Double layer in ionic liquids: overscreening versus crowding. *Phys. Rev. Lett.* **2011**, *106* (4), 046102.
60. Avni, Y.; Adar, R. M.; Andelman, D. Charge oscillations in ionic liquids: A microscopic cluster model. *Phys. Rev. E* **2020**, *101* (1−1), 010601.
61. Limmer, D. T. Interfacial ordering and accompanying divergent capacitance at ionic liquid-metal interfaces. *Phys. Rev. Lett.* **2015**, *115* (25), 256102.
62. Gavish, N.; Yochelis, A. Theory of Phase Separation and Polarization for Pure Ionic Liquids. *J. Phys. Chem. Lett.* **2016**, *7* (7), 1121–1126.
63. de Souza, J. P.; Goodwin, Z. A. H.; McEldrew, M.; Kornyshev, A. A.; Bazant, M. Z. Interfacial Layering in the Electric Double Layer of Ionic Liquids. *Phys. Rev. Lett.* **2020**, *125* (11), 116001.
64. Rosenfeld, Y. Free-energy model for the inhomogeneous hard-sphere fluid mixture and density-functional theory of freezing. *Phys. Rev. Lett.* **1989**, *63* (9), 980–983.
65. de Souza, J. P.; Pivnic, K.; Bazant, M. Z.; Urbakh, M.; Kornyshev, A. A. Structural Forces in Ionic Liquids: The Role of Ionic Size Asymmetry. *J. Phys. Chem. B* **2022**, *126* (6), 1242–1253.

66. Misra, R. P.; de Souza, J. P.; Blankschtein, D.; Bazant, M. Z. Theory of Surface Forces in Multivalent Electrolytes. *Langmuir* **2019**, *35* (35), 11550–11565.
67. Lee, A. A.; Vella, D.; Perkin, S.; Goriely, A. Are Room-Temperature Ionic Liquids Dilute Electrolytes? *J. Phys. Chem. Lett.* **2015**, *6* (1), 159–163.
68. Chen, M.; Goodwin, Z. A. H.; Feng, G.; Kornyshev, A. A. On the temperature dependence of the double layer capacitance of ionic liquids. *J. Electroanal. Chem.* **2018**, *819*, 347–358.
69. Ma, K.; Forsman, J.; Woodward, C. E. Influence of ion pairing in ionic liquids on electrical double layer structures and surface force using classical density functional approach. *J. Chem. Phys.* **2015**, *142* (17), 174704.
70. Goodwin, Z. A.; McEldrew, M.; Kozinsky, B.; Bazant, M. Z. Theory of Cation Solvation and Ionic Association in Non-Aqueous Solvent Mixtures. *PRX Energy* **2023**, *2*, 013007.
71. Goodwin, Z. A. H.; Kornyshev, A. A. Underscreening, overscreening and double-layer capacitance. *Electrochem. Commun.* **2017**, *82*, 129–133.
72. Feng, G.; Chen, M.; Bi, S.; Goodwin, Z. A. H.; Postnikov, E. B.; Brilliantov, N.; Urbakh, M.; Kornyshev, A. A. Free and Bound States of Ions in Ionic Liquids, Conductivity, and Underscreening Paradox. *Phys. Rev. X* **2019**, *9* (2), 021024.
73. Lee, A. A.; Perez-Martinez, C. S.; Smith, A. M.; Perkin, S. Underscreening in concentrated electrolytes. *Faraday Discuss.* **2017**, *199* (0), 239–259.
74. Adar, R. M.; Safran, S. A.; Diamant, H.; Andelman, D. Screening length for finite-size ions in concentrated electrolytes. *Phys. Rev. E* **2019**, *100* (4-1), 042615.
75. Rotenberg, B.; Bernard, O.; Hansen, J. P. Underscreening in ionic liquids: a first principles analysis. *J. Phys. Condens. Matter* **2018**, *30* (5), 054005.
76. Coupette, F.; Lee, A. A.; Hartel, A. Screening Lengths in Ionic Fluids. *Phys. Rev. Lett.* **2018**, *121* (7), 075501.
77. Krucker-Velasquez, E.; Swan, J. W. Underscreening and hidden ion structures in large scale simulations of concentrated electrolytes. *J. Chem. Phys.* **2021**, *155* (13), 134903.
78. Zeman, J.; Kondrat, S.; Holm, C. Bulk ionic screening lengths from extremely large-scale molecular dynamics simulations. *Chem. Commun. (Cambridge, U. K.)* **2020**, *56* (100), 15635–15638.
79. McEldrew, M.; Goodwin, Z. A. H.; Molinari, N.; Kozinsky, B.; Kornyshev, A. A.; Bazant, M. Z. Salt-in-Ionic-Liquid Electrolytes: Ion Network Formation and Negative Effective Charges of Alkali Metal Cations. *J. Phys. Chem. B* **2021**, *125* (50), 13752–13766.
80. Goodwin, Z. A. H.; Kornyshev, A. A. Cracking Ion Pairs in the Electrical Double Layer of Ionic Liquids. *Electrochim. Acta* **2022**, *434*, 141163.
81. Goodwin, Z. A. H.; McEldrew, M.; Pedro de Souza, J.; Bazant, M. Z.; Kornyshev, A. A. Gelation, clustering, and crowding in the electrical double layer of ionic liquids. *J. Chem. Phys.* **2022**, *157* (9), 094106.
82. Ueno, K.; Inaba, A.; Kondoh, M.; Watanabe, M. Colloidal stability of bare and polymer-grafted silica nanoparticles in ionic liquids. *Langmuir* **2008**, *24* (10), 5253–5259.
83. Ueno, K.; Watanabe, M. From colloidal stability in ionic liquids to advanced soft materials using unique media. *Langmuir* **2011**, *27* (15), 9105–9115.
84. Szilagyi, I.; Szabo, T.; Desert, A.; Trefalt, G.; Oncsik, T.; Borkovec, M. Particle aggregation mechanisms in ionic liquids. *Phys. Chem. Chem. Phys.* **2014**, *16* (20), 9515–9524.

85. Takács, D.; Tomšič, M.; Szilagyi, I. Effect of water and salt on the colloidal stability of latex particles in ionic liquid solutions. *Colloids Interfaces* **2022**, *6* (1), 2.
86. Katana, B.; Takács, D.; Bobbink, F. D.; Dyson, P. J.; Alsharif, N. B.; Tomšič, M.; Szilagyi, I. Masking specific effects of ionic liquid constituents at the solid–liquid interface by surface functionalization. *Phys. Chem. Chem. Phys.* **2020**, *22* (42), 24764–24770.
87. Jitvisate, M.; Seddon, J. R. T. Direct Measurement of the Differential Capacitance of Solvent-Free and Dilute Ionic Liquids. *J. Phys. Chem. Lett.* **2018**, *9* (1), 126–131.
88. Suo, L.; Borodin, O.; Gao, T.; Olguin, M.; Ho, J.; Fan, X.; Luo, C.; Wang, C.; Xu, K. "Water-in-salt" electrolyte enables high-voltage aqueous lithium-ion chemistries. *Science* **2015**, *350* (6263), 938–943.
89. McEldrew, M.; Goodwin, Z. A. H.; Bi, S.; Kornyshev, A. A.; Bazant, M. Z. Ion Clusters and Networks in Water-in-Salt Electrolytes. *J. Electrochem. Soc.* **2021**, *168* (5), 050514.
90. Borodin, O.; Suo, L.; Gobet, M.; Ren, X.; Wang, F.; Faraone, A.; Peng, J.; Olguin, M.; Schroeder, M.; Ding, M. S.; Gobrogge, E.; von Wald Cresce, A.; Munoz, S.; Dura, J. A.; Greenbaum, S.; Wang, C.; Xu, K. Liquid Structure with Nano-Heterogeneity Promotes Cationic Transport in Concentrated Electrolytes. *ACS Nano* **2017**, *11* (10), 10462–10471.
91. Zhang, R.; Han, M.; Ta, K.; Madsen, K. E.; Chen, X.; Zhang, X.; Espinosa-Marzal, R. M.; Gewirth, A. A. Potential-Dependent Layering in the Electrochemical Double Layer of Water-in-Salt Electrolytes. *ACS Appl. Energy Mater.* **2020**, *3* (8), 8086–8094.
92. Espinosa-Marzal R. M., Goodwin Z. A. H., Zhang X., Zheng Q. Colloidal Interactions in Ionic Liquids–the electrical double layer inferred from ion layering and aggregation. *ChemRxiv*; Cambridge Open Engage: Cambridge, 2023. This content is a preprint and has not been peer-reviewed.